

Do triaxial supramassive compact stars exist?

Kōji Uryū,¹ Antonios Tsokaros,² Luca Baiotti,³ Filippo Galeazzi,²
Noriyuki Sugiyama,⁴ Keisuke Taniguchi,¹ and Shin'ichirou Yoshida⁵

¹*Department of Physics, University of the Ryukyus, Senbaru, Nishihara, Okinawa 903-0213, Japan*

²*Institut für Theoretische Physik, Johann Wolfgang Goethe-Universität,
Max-von-Laue-Strasse 1, 60438 Frankfurt am Main, Germany*

³*Graduate School of Science, Osaka University, 560-0043 Toyonaka, Japan*

⁴*Department of Mathematical Sciences, University of Wisconsin-Milwaukee, Milwaukee, Wisconsin 53211*

⁵*Department of Earth Science and Astronomy, Graduate School of Arts and Sciences,
The University of Tokyo, Komaba, Tokyo 153-8902, Japan*

(Dated: September 2, 2018)

We study quasiequilibrium solutions of triaxially deformed rotating compact stars – a generalization of Jacobi ellipsoids under relativistic gravity and compressible equations of state (EOS). For relatively stiff (piecewise) polytropic EOSs, we find supramassive triaxial solutions whose masses exceed the maximum mass of the spherical solution, but are always lower than those of axisymmetric equilibria. The difference in the maximum masses of triaxial and axisymmetric solutions depends sensitively on the EOS. If the difference turns out to be only about 10%, it will be strong evidence that the EOS of high density matter becomes substantially softer in the core of neutron stars. This finding opens a novel way to probe phase transitions of high density nuclear matter using detections of gravitational waves from new born neutron stars or magnetars under fallback accretion.

Introduction.—Maclaurin spheroids and Jacobi ellipsoids, classical solutions of self-gravitating and uniformly rotating incompressible fluids in equilibrium, are the first two models of rapidly rotating stars. As the rotation of an equilibrium configuration is increased, a sequence of triaxial Jacobi ellipsoids branches off from that of axisymmetric Maclaurin spheroids where the ratio of kinetic to gravitational energies reach $T/|W| \sim 0.14$ (see, e.g. [1]). This led to historical mathematical studies including Poincaré's bifurcation theory [2]. A generalization of the Maclaurin spheroids, and other stationary axisymmetric equilibria, to the case of relativistic gravity have been fully investigated in [3]. From a point of view of relativistic astrophysics, it is also important to include compressibility of the fluid; realistic neutron stars are modeled as axisymmetric and uniformly rotating configurations associated with equations of state (EOSs) of high density nuclear matter (see e.g. [4, 5]).

It is not so surprising that a relativistic generalization of Jacobi ellipsoids, even for the case with compressible fluid, has been of little astrophysical interest, because of the following four difficulties. Firstly, such non-axisymmetric, triaxially deformed, solutions can not be stationary equilibria due to the back reaction of gravitational waves [6, 7].¹ Secondly, there should be a highly efficient mechanism to spin up the compact star as fast as $T/|W| \sim 0.14$. Thirdly, in realistic high density nuclear matter, the viscosity may not be strong enough

to bring a flow field to uniform rotation within a time scale shorter than the time scale of gravitational radiation [6, 7]. Fourthly, even in Newtonian gravity, such a triaxial sequence does not exist for the gaseous EOSs unless the EOS is stiff enough. For the case with polytropic EOS, $p = K\rho^\Gamma$, the triaxial sequence only exists in the range $\Gamma \gtrsim 2.24$, where p is the gas pressure, ρ the (rest mass) density, K the adiabatic constant, and Γ the adiabatic index [8]. Even for such stiff EOS, say $2.24 \lesssim \Gamma \lesssim 4$, the triaxial sequence is terminated at the mass shedding limit not very far away from the branching point as its angular momentum is increased [9].

Although a couple of Kuiper Belt objects are likely to rotate rapidly enough to become Jacobi ellipsoids [10], it is still inconclusive whether such triaxially deformed rapidly rotating configuration is realized or not for compact objects such as neutron stars. However, the last two difficulties above may be avoided. There are various types of phenomenologically derived high density nuclear matter EOSs, some of which may be approximated fairly accurately by polytropic or better by piecewise polytropic EOSs with Γ as large as $\Gamma \sim 3 - 4$ [11]. Viscosity of neutron star matter, which is normally expected to be weak, may be enhanced by magnetic effects and/or high temperature [12].

Moreover, in a recent paper [13], Piro and Ott have shown that the supernova fallback accretion may spin up a newly formed neutron star associated with the strong magnetic field $B \lesssim 5 \times 10^{14}$ G as fast as the above criteria $T/|W| \sim 0.14$ for $\sim 50 - 200$ s until the star collapses to a black hole. Therefore, there is a possibility that such triaxially deformed compact stars may be formed transiently after massive stellar core collapses. Once such triaxial star is formed, the amount of gravitational wave

¹ Hereafter we use a term 'triaxially deformed' or simply 'triaxial' star rather than 'ellipsoid', since the configurations are no longer an exact ellipsoid in relativistic gravity or for compressible fluids. The triaxial configurations in this paper possess the tri-planar symmetry with respect to three orthogonal x, y, and z planes.

emission is enormous, from which we could extract properties of high density nuclear matter. Piro and Thrane have estimated the detectability of gravitational waves from triaxially deformed compact stars within the fallback accretion scenario for the case of the advanced LIGO detector [15] as ~ 17 Mpc using a realistic excess cross-power search algorithm [16].² This scenario motivates us to further investigate the properties of triaxially deformed compact stars.³

In our previous calculations [17, 18], it was apparent that the triaxial sequence becomes shorter (that is, a smaller deformation is allowed) for the case with higher compactness. For certain EOSs, it is even unclear whether there exist supramassive triaxial solutions whose masses are higher than the maximum mass of the spherically symmetric solutions of Tolman-Oppenheimer-Volkov (TOV) equations, just like the case for axisymmetric uniformly rotating solutions. In this letter, we present for the first time a systematic study of the classical problem for computing triaxially deformed uniformly rotating stars in general relativistic gravity, and elucidate the properties of the quasiequilibrium sequences of such rotating stars for (piecewise) polytropic EOSs up to their maximum mass.

A method for computing sequences of solutions.— We focus on computing rotating compact stars for three EOSs. Two of them are polytropic EOSs $p = K\rho^\Gamma$ with adiabatic constant $\Gamma = 3$ or 4, and the other is a two segments piecewise polytropic EOS $p = K_i\rho^{\Gamma_i}$ ($i = 1, 2$), with $\Gamma_1 = 4$ for $\rho \leq 2\rho_{\text{nuc}}$ and $\Gamma_2 = 2.5$ for $\rho > 2\rho_{\text{nuc}}$. We set the interface value of the rest mass density ρ_{nuc} to be the nuclear saturation density $\rho_{\text{nuc}} = 2.8 \times 10^{14} \text{g/cm}^3$ in cgs unit. We choose the value of the adiabatic constant K and K_i so that the value of the rest mass M_0 becomes $M_0 = 1.5M_\odot$ at the compactness $M/R = 0.2$ for the TOV solution. Physical quantities of spherically symmetric solutions at the maximum mass of these EOSs are presented in Table I.⁴

The most accurate rotating triaxial equilibriums of

Γ	$(p/\rho)_c$	ρ_c	M_0	M	M/R
3	0.827497	0.00415972	2.24295	1.84989	0.316115
4	1.330409	0.00322082	2.88207	2.24967	0.355062
(4, 2.5)	0.568330	0.00454117	1.96013	1.65738	0.287213

TABLE I. Quantities at the maximum mass of spherically symmetric solutions are listed for the polytropic EOSs $p = K\rho^\Gamma$ with $\Gamma = 3$ and 4, and for the two segments piecewise polytropic EOS $p = K_i\rho^{\Gamma_i}$ with $(\Gamma_1, \Gamma_2) = (4, 2.5)$. The adiabatic constant K and K_i are chosen so that the value of the rest mass M_0 becomes $M_0 = 1.5$ at the compactness $M/R = 0.2$.^a Note that the last EOS $(\Gamma_1, \Gamma_2) = (4, 2.5)$ is softer than the others. Values are in $G = c = M_\odot = 1$ unit, and are approximated using 2nd order interpolation of nearby 3 solutions. To convert the units of the central density ρ_c to cgs, multiply by $M_\odot(GM_\odot/c^2)^{-3} \approx 6.176393 \times 10^{17} \text{g cm}^{-3}$.

^a For the relativistic (piecewise) polytropes, physical dimensions enter only through the constant K . Dimensionless values of mass and radius are obtained from dividing each by a factor $K^{1/2(\Gamma-1)}$ in $G = c = 1$ unit.

compact stars would be computed as helically symmetric solutions associated with standing gravitational waves. One can, however, truncate the gravitational-wave content because its contribution to the source's equilibrium is small, and instead compute quasiequilibrium initial data on a three dimensional hypersurface. We have developed a code for computing such data as a part of our Compact Object CALculator COCAL code [18, 19]. To reduce computing time, we use the Isenberg-Wilson-Mathews formulation in this paper. Further details on the numerical method, as well as the definitions on physical quantities, are found in [18].

For each EOS and for both axisymmetric and triaxial configurations, we compute sequences of solutions varying two parameters which determine the compactness (or the mass) and the degree of rotation. In practice, for the former, we choose the central density ρ_c , and for the latter, the axis ratio (deformation) R_z/R_x for the axisymmetric solutions, and R_y/R_x for the triaxial solutions, where R_x , R_y , R_z are the radii along the semi-major axis. The z -axis corresponds to the axis of rotation, and the x -axis is along the longest semi-principal axis for the case of triaxial solutions. For each deformation model, a sequence of solutions is calculated with increasing ρ_c , typically from $\rho_c = 3.0 \times 10^{14} \text{g/cm}^3$ to $3.0 \times 10^{15} \text{g/cm}^3$. As ρ_c is increased, these sequences with the fixed deformation may or may not be terminated at the mass-shedding limit before ρ_c reaches $3.0 \times 10^{15} \text{g/cm}^3$. As far as our selected EOS models are concerned, the triaxial sequences with fixed R_y/R_x and increasing ρ_c are always terminated at the mass shedding limit, while the axisymmetric sequences are terminated at the mass shedding limit only for the smaller R_z/R_x (larger deformation) cases.

Results.— In Fig. 1, the rest mass M_0 is plotted with respect to the square of eccentricity in proper length $e^2 := 1 - (\bar{R}_z/\bar{R}_x)^2$ for the above three EOS models.

² The amplitude of gravitational waves from triaxial stars is typically [14],

$$h \sim 9.1 \times 10^{-21} \left(\frac{30 \text{ Mpc}}{D} \right) \left(\frac{M}{1.4M_\odot} \right)^{3/4} \left(\frac{R}{10 \text{ km}} \right)^{1/4} f^{-1/5},$$

where D , M , R , and f are, respectively, the distance to the source, the source mass, the mean radius, and the wave frequency in Hz.

³ A magnetic field $B \lesssim 5 \times 10^{14} \text{G}$ is not strong enough to alter the hydrostatic equilibrium of rotating compact stars.

⁴ The adiabatic speed of sound $c_s := \sqrt{dp/d\epsilon}$ for the polytropic EOSs with $\Gamma = 3$ and 4 exceeds the speed of light when the rest mass density $\rho/\rho_c \gtrsim 0.898$ and 0.656, where values of ρ_c are tabulated in Table I for $\Gamma = 3$ and 4, respectively. The results from these acausal EOSs for $\Gamma = 3$ and 4 are shown for a comparison with our piecewise polytropic EOS model with $(\Gamma_1, \Gamma_2) = (4, 2.5)$ which is always causal in the range of ρ calculated in this letter.

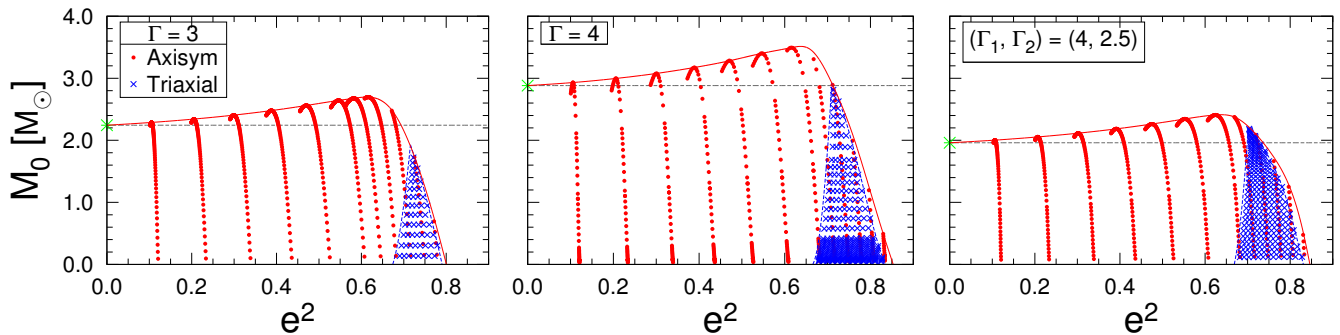


FIG. 1. The rest mass M_0 is plotted against the square of the eccentricity (in proper length) $e^2 := 1 - (\bar{R}_z/\bar{R}_x)^2$ for axisymmetric (red dots) and triaxial (blue crosses) solutions of uniformly rotating compact stars. Solid (red) and dashed (blue) envelope curves are polynomial fits to the extrapolated limiting solutions. Left to right panels correspond to the results of polytropic EOS $\Gamma = 3$ and 4, and piecewise polytropic EOS $(\Gamma_1, \Gamma_2) = (4, 2.5)$, respectively. Solutions above the horizontal dashed line in each panel are supramassive, $M_0 > M_{\text{max}}^{\text{SPH}}$. In each panel, the left fitted curve to the triaxial solutions (blue dashed) corresponds to the bifurcation points, and the right to the mass shedding (Roche) limits.

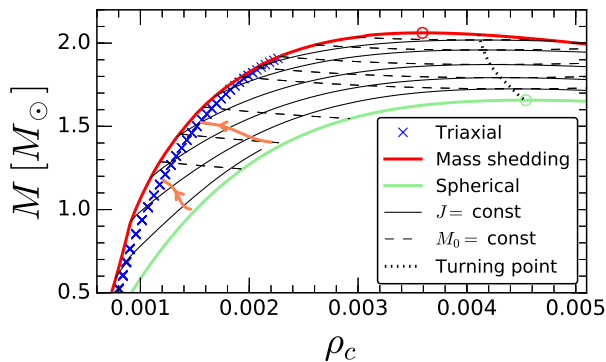


FIG. 2. The gravitational (Arnowitt-Deser-Misner) mass M is plotted against the central density ρ_c for the same model with the right panel of Fig. 1, $(\Gamma_1, \Gamma_2) = (4, 2.5)$. Solid and dashed curves are axisymmetric sequences with $J = \text{constant}$, and $M_0 = \text{constant}$, respectively. Turning points of these curves are indicated by a dotted curve. Top (red) and bottom (green) circles are the maximum of the gravitational mass for the axisymmetric and spherical stars, respectively. For a reference, we draw evolutionary tracks (thick curves with arrows) of newly born magnetars under the fallback accretion modeled by Piro and Ott Eqs. (14)-(16) in [13]. For simplicity, a spin equilibrium (Eq. (17) in [13]) is always assumed.

A cross point on the vertical axis at $e^2 = 0$ in each panel indicates the maximum rest mass of a spherically symmetric solution for each EOS model tabulated in Table I. We notice that, for the case with $\Gamma = 3$, the maximum mass of triaxial solutions never exceeds that of the spherical solutions. For the $\Gamma = 4$ case, the mass of all computed triaxial solutions again does not exceed that of the spherical solutions. However, if we extrapolate the triaxial solutions closer towards the axisymmetric solution (a peak of dashed curves), we could find triaxial

solutions with mass higher than the maximum mass of the spherical solutions. Therefore, we may conclude that supramassive triaxial solutions exist for $\Gamma \gtrsim 4$, although the excess of mass is much lower than that of axisymmetric supramassive solutions.

It is important to notice that the deformation sequence of triaxial solutions with a constant rest mass M_0 becomes shorter for more massive (higher compactness) models, and hence the maximum mass of the triaxial solutions can be found in the vicinity of the bifurcation point of the axisymmetric and triaxial sequences. This is due to the fact that the density distribution becomes more centrally condensed as the relativistic star becomes more compact, and hence the mass shedding limit of $M_0 = \text{constant}$ sequence (where the matter at the equator (or at the largest radius for the case with the triaxial solution) brakes up) appears at a smaller deformation (R_y/R_x closer to unity).⁵ Hereafter, we denote the maximum rest mass of the spherical solutions, the rotating axisymmetric sequences, and the rotating triaxial sequences by $M_{\text{max}}^{\text{SPH}}$, $M_{\text{max}}^{\text{AX}}$, and $M_{\text{max}}^{\text{TR}}$, respectively.

For the piecewise polytrope model with $(\Gamma_1, \Gamma_2) = (4, 2.5)$ one might expect that, since the value of Γ_2 of this EOS is substantially lower than the $\Gamma = 4$ polytrope, $M_{\text{max}}^{\text{TR}}$ for this EOS may become lower than $M_{\text{max}}^{\text{SPH}}$ as in the case with $\Gamma = 3$. The right panel of Fig. 1 shows that it is not the case; the supramassive triaxial solutions for the $(\Gamma_1, \Gamma_2) = (4, 2.5)$ EOS do clearly exist. For axisymmetric solutions, $M_{\text{max}}^{\text{AX}}$ exceeds $M_{\text{max}}^{\text{SPH}}$ for each EOS around 20%: for the computed solutions in Fig. 1, the excesses are 20.2%, 21.2%, and 22.8% for $\Gamma = 3$, $\Gamma = 4$,

⁵ This is analogous to Newtonian rotating stars; for softer and more centrally condensed EOSs, rotating equilibria reach the brake up velocity (Roche limit) with a smaller deformation.

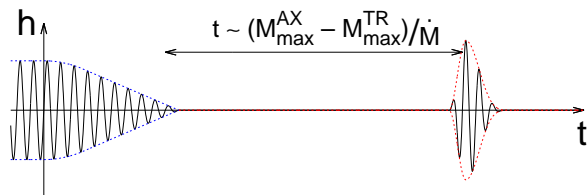


FIG. 3. An illustrative gravitational waveform from a compact star under fallback accretion. A diminishing periodic wave from a triaxially deformed rotating star is followed by a burst wave from a collapse.

and $(\Gamma_1, \Gamma_2) = (4, 2.5)$, respectively. On the other hand, the calculated M_{\max}^{TR} in Fig. 1, which appears close to the bifurcation point, falls behind M_{\max}^{SPH} by -23.2% and -2.41% for $\Gamma = 3$ and $\Gamma = 4$, respectively, while it exceeds 11.5% for the $(\Gamma_1, \Gamma_2) = (4, 2.5)$ case.

This striking difference in the behavior between M_{\max}^{AX} and M_{\max}^{TR} can be understood qualitatively as follows. In Fig. 1, each consecutive point from smaller to larger M_0 in (e^2, M_0) plane corresponds to a sequence $M_0(\rho_c)$ with a fixed axis ratio (and varying ρ_c). For the axisymmetric solutions with $e^2 \lesssim 0.7$, each sequence has a turning point where M_0 reaches the maximum and then decrease as ρ_c increases. This is related to a change of stability associated with the fundamental (F) mode [4]. As shown in Fig. 2 for the case with $(\Gamma_1, \Gamma_2) = (4, 2.5)$, simultaneous turning points appear on $M(\rho_c)$ curves with constant M_0 and J , where M is the gravitational (Arnowitt-Deser-Misner) mass. There, the axisymmetric configurations become radially unstable, just like a stability change at the maximum mass of spherical stars M_{\max}^{SPH} [20, 21].⁶

The fact that the sequences $e^2 \gtrsim 0.7$ in Fig.1 are without turning points suggests that these solutions are not subject to radial instability, and the sequences $M_0(\rho_c)$ with fixed axis ratio terminate at the mass shedding (Roche) limit. The maximum mass of the (supramassive) axisymmetric uniformly rotating solutions M_{\max}^{AX} in our definition is expected to appear near this turning point and the Roche limit merge. M_{\max}^{AX} is, hence, associated with the radial instability, and this excess of $\sim 20\%$ from M_{\max}^{SPH} turned out to be almost independent on the EOS for the uniformly rotating case. In contrast, M_{\max}^{TR} is not related to the radial instability limit but to the Roche limit in the range of the adiabatic index we are interested in. The Roche limit is sensitive to the stiffness of

the EOS: the stiffer EOSs in the lower density region, say $\rho < 2\rho_{\text{nuc}}$, prevent mass shedding to occur.

Therefore, if, as in certain models of realistic neutron star EOSs, the EOS is softer for higher densities (inner core), and is stiffer for lower densities (outer core), supra-massive triaxial neutron stars are formed.

Discussion.—In [13], it is demonstrated that the accretion rate of fall back material to a new born strongly magnetized neutron star in the supernova remnant can be as high as $\dot{M} \sim 10^{-4}$ - $10^{-2} M_{\odot}/\text{s}$ and transport enough angular momentum to spin up the neutron star and to cause the onset of a non-axisymmetric instability (see, Fig.2). Assuming the accretion rate to be constant at this rate, we expect that the star stays at the temperature, T , of the order of $T \sim 10^9 \text{K}$, because of the continuous emission of thermal neutrinos [23]. At such high temperature, the bulk viscosity of neutron star matter dominates over the shear viscosity as their temperature dependences are $\propto T^6$ and $\propto T^{-2}$ for the bulk and shear, respectively. The bulk viscosity also dominates over the gravitational waves so that it drives the star to a non-axisymmetric figure – establishing a Jacobi-like configuration [12].

Detectability of gravitational waves from such accreting neutron stars (or magnetars) has been discussed in [16], in which the gravitational waveform is modeled as periodic waves from Jacobi ellipsoids with increasing mass. This scenario is modified for the case with compressible EOS. Our finding suggests that the periodic gravitational wave signal from triaxially deformed neutron stars would be terminated at the time when the mass approaches M_{\max}^{TR} . It is likely that the accretion continues with the same rate after the disappearance of the periodic signal as the mass increases beyond M_{\max}^{TR} . Then, within 10-1000s, we expect a gravitational wave burst, or a prompt emission of some electromagnetic signal from the collapse of the axisymmetric neutron star to form a black hole as the mass grows over M_{\max}^{AX} .

Modeling of the waveform from such an accreting triaxial compact star, which may look like the one in Fig. 3, is beyond our scope in this letter. However, we stress the qualitative importance of the detection of such gravitational waves and its implication for the EOS of the high temperature side of the high density neutron star matter. From the data analysis of periodic gravitational waves emitted from the accreting triaxially deformed neutron stars, we could determine the maximum mass of the triaxial solution M_{\max}^{TR} (which may or may not be supra-massive) and the mass accretion rate \dot{M} . The maximum mass of the axisymmetric supra-massive solution M_{\max}^{AX} may also be determined from the duration between the disappearance and the burst of gravitational wave signals (or from the burst waveform itself). The time until a collapse to form a BH may be detected also through other electromagnetic signals. And most importantly, the gap between these two signals carries clear information on the EOS of high density neutron star matter. If the value of

⁶ The criteria is known to be a sufficient condition for stability, and recent simulations suggest that the vanishing F-mode appears somewhat smaller ρ_c than that determined by the turning point method [4, 22]. Because the point where the stability changes is placed beyond the maximum mass M_{\max}^{AX} , the difference between M_{\max}^{AX} and the mass at the radial stability limit does not affect our discussion.

M_{\max}^{AX} turned out to be only about 10% larger than M_{\max}^{TR} , it would be strong evidence for the fact that the EOS of high density neutron star matter is substantially softer in the core of neutron stars.

It should be noted that our (piecewise) polytropic EOS is understood as a parametrization of various types of nuclear EOS. A variety of microphysics of high density nuclear matter can be integrated into the adiabatic indices Γ_i , the dividing densities at the interfaces of successive segments, and an adiabatic constant of one of segments. As demonstrated in [11], it is a best practice to introduce such piecewise polytropic EOS with a minimal number of segments to parametrize realistic EOSs to constrain them through gravitational wave observations. However, according to [11] for the case with binary neutron star inspirals, one EOS parameter may be constrained from the gravitational wave observations by advanced LIGO detectors, and two by Einstein Telescope (but those could be improved by optimizing a detector sensitivity).

The stiffness of the EOS is the essential property affecting the maximum masses, and in our two segment piecewise polytropic EOS model that is parametrized by the (Γ_1, Γ_2) of the outer and inner cores. Then, the possibilities are whether (i) the stiffness is approximately the same for inner and outer cores, $\Gamma_1 \approx \Gamma_2$, (ii) the inner core is stiffer than the outer core, $\Gamma_1 < \Gamma_2$, or (iii) the inner core is softer than the outer core, $\Gamma_1 > \Gamma_2$, and the stiffness of the outer core Γ_1 may be compared with $\Gamma \sim 2.5 - 3$ where the relativistic triaxial solutions appear. The case (i) is the same as a simple (one segment) polytropic EOS: a difference between axisymmetric and triaxial maximum masses defined by $\Delta M_{\max} := (M_{\max}^{\text{AX}} - M_{\max}^{\text{TR}})/M_{\max}^{\text{SPH}}$ will depend systematically on the indices Γ_i . The maximum mass difference ΔM_{\max} for the case (i) will be larger than $\Delta M_{\max} \gtrsim 20\%$ in a range $2.24 \lesssim \Gamma \lesssim 4$ (and supposedly in $\Gamma \gtrsim 4$ also). For the case (ii), ΔM_{\max} can not be smaller than the case (i) because the maximum mass of spherical and axisymmetric solutions, M_{\max}^{SPH} and M_{\max}^{AX} , are not affected by the EOS of the outer core but mostly by the inner core [11], while the maximum mass of triaxial star M_{\max}^{TR} becomes smaller for the softer EOS in the outer core. Hence ΔM_{\max} will be the same or larger than 20% for the case (ii).

Therefore it seems legitimate to conclude that the maximum mass difference ΔM_{\max} will be less than 10% for outer core's $\Gamma_1 \approx 4$, and inner core's $\Gamma_2 \lesssim 2.5$, and as considering the systematic dependence of the maximum masses on the stiffness of EOS, ΔM_{\max} would be around 10% or less for the other combination of Γ_i , such as $\Gamma_1 \approx 3.5$ and $\Gamma_2 \lesssim 2$ for the outer and inner cores, respectively. As an example, apart from the results presented in the previous section, we have also calculated a case with $(\Gamma_1, \Gamma_2) = (3.5, 2.5)$, and found the mass difference to be $\Delta M_{\max} = 15.4\%$. Clearly, such modifications in Γ_i do not change the above statement, that the mass

difference $\Delta M_{\max} \lesssim 10\%$ is a strong evidence for the softer inner core and stiffer outer core.

The illustrative waveform in Fig. 3 may be different from the actual wave form, because such compact rapidly rotating stars are also unstable to the Chandrasekhar-Friedman-Schutz (CFS) mechanism [4, 6, 24], which sets in at a value of $T/|W|$ lower than that of the dominant viscosity-driven secular $\ell = m = 2$ f-mode [25]. Therefore, after M_{\max}^{TR} is reached, we might still see the signals of lower order gravitational f-modes ($m = 2-4$) and/or r-modes [26]. Such modes are assumed to be suppressed in the above scenario because of a strong viscosity mechanism or turbulent magnetic flow. If not, the modeling of the waveform becomes more challenging.

Because of the recent successful detection of gravitational waves from a binary black hole merger, the detection of those from neutron stars looks very promising [27]. Since the above signal from triaxial compact star resides roughly around 2000-3000Hz for a compactness $M/R \sim 0.2-0.3$ [28], it will be necessary to improve the sensitivity in this bandwidth using narrow banding [29].

This work was supported by JSPS Grant-in-Aid for Scientific Research(C) 15K05085, 25400262, 26400267, and 26400274.

-
- [1] S. Chandrasekhar, "Ellipsoidal Figures of Equilibrium", (Yale University, New Haven, 1969); I. Hachisu, I., and Y. Eriguchi, Publ. Astron. Soc. Japan 36, 497 (1984)
 - [2] H. Poincaré, *Figures D'Équilibre D'Une Masse Fluide*, Paris (1902); H. Lamb, *Hydrodynamics* (6th ed.) Chap. 12, Cambridge University Press, UK (1932)
 - [3] R. Meinel, M. Ansorg, A. Kleinwächter, G. Neugebauer, and D. Petroff, *Relativistic Figures of Equilibrium*, Cambridge University Press, New York (2008).
 - [4] J. L. Friedman and N. Stergioulas, *Rotating Relativistic Stars*, Cambridge University Press, Cambridge, UK, 2013;
 - [5] N. Straumann, *General Relativity*, Springer Science+Business Media Dordrecht, 2013;
 - [6] S. Chandrasekhar, Phys. Rev. Lett. **24**, 611 (1970).
 - [7] B. Miller, ApJ 181, 497 (1973); S. L. Detweiler, and L. Lindblom, ApJ 213, 193 (1977); L. Lindblom, S. L. Detweiler, ApJ 211, 565 (1977).
 - [8] R. A. James, Astrophys. J. 140, 552 (1964)
 - [9] I. Hachisu, and Y. Eriguchi, Prog. Theor. Phys. 68, 206 (1982); D. Lai, F. A. Rasio, and S. L. Shapiro, Astrophys. J. Suppl. 88, 205 (1993)
 - [10] D. L. Rabinowitz, K. Barkume, M. E. Brown, et.al., Astrophys. J., 639, 1238 (2006); P. Lacerda, and D. C. Jewitt, Astron. J., 133, 1393 (2007)
 - [11] J. S. Read, B. D. Lackey, B. J. Owen and J. L. Friedman, Phys. Rev. D **79**, 124032 (2009); J. S. Read, C. Markakis, M. Shibata, K. Uryu, J. D. E. Creighton and J. L. Friedman, Phys. Rev. D **79**, 124033 (2009)
 - [12] C. Cutler and L. Lindblom, Astrophys. J., 314, 234 (1987); R. F. Sawyer, Phys. Rev. D **39**, 3804 (1989).
 - [13] A. L. Piro, and C. D. Ott, Astrophys. J. 736, 108 (2011);

- [14] D. Lai and S. L. Shapiro, *Astrophys. J.* **442**, 259 (1995)
- [15] G. M. Harry [LIGO Scientific Collaboration], *Class. Quant. Grav.* **27**, 084006 (2010).
- [16] A. L. Piro, and E. Thrane, *Astrophys. J.* **761**, 63 (2012)
- [17] X. Huang, C. Markakis, N. Sugiyama and K. Uryu, *Phys. Rev. D* **78**, 124023 (2008);
- [18] K. Uryu, A. Tsokaros, F. Galeazzi, H. Hotta, M. Sugimura, K. Taniguchi and S. i. Yoshida, *Phys. Rev. D* **93**, no. 4, 044056 (2016).
- [19] K. Uryu and A. Tsokaros, *Phys. Rev. D* **85**, 064014 (2012) K. Uryu, A. Tsokaros and P. Grandclement, *Phys. Rev. D* **86**, 104001 (2012) ; A. Tsokaros and K. Uryū, *J. Eng. Math.* **82**, 133 (2013).
- [20] J. L. Friedman, J. R. Ipser and R. D. Sorkin, *Astrophys. J.* **325**, 722 (1988).
- [21] G. B. Cook, S. L. Shapiro and S. A. Teukolsky, *Astrophys. J.*, **398**, 203 (1992); G. B. Cook, S. L. Shapiro and S. A. Teukolsky, *Astrophys. J.*, **422**, 227 (1994); G. B. Cook, S. L. Shapiro and S. A. Teukolsky, *Astrophys. J.* **424**, 823 (1994);
- [22] K. Takami, L. Rezzolla and S. Yoshida, *Mon. Not. Roy. Astron. Soc.* **416**, L1 (2011)
- [23] S. Yoshida, and Y. Eriguchi, *Mon. Not. Roy. Astron. Soc.* **316**, 917 (2000)
- [24] J. L. Friedman and B. F. Schutz, *Astrophys. J.Lett.*, **199**, L157 (1975); J. L. Friedman and B. F. Schutz, *Astrophys. J.*, **200**, 204 (1975)
- [25] N. Comins, *Mon. Not. Roy. Astron. Soc.* **189**, 255 (1979); C. Cutler, and L. Lindblom, *Astrophys. J.*, **314**, 234 (1987)
- [26] N. Andersson, and K. D. Kokkotas, *Mon. Not. Roy. Astron. Soc.* **299**, 1059 (1998)
- [27] B. P. Abbott *et al.* [LIGO Scientific and Virgo Collaborations], *Phys. Rev. Lett.* **116**, no. 6, 061102 (2016)
- [28] M. Saijo and E. Gourgoulhon, *Phys. Rev. D* **74**, 084006 (2006)
- [29] S. A. Hughes, *Phys. Rev. D* **66**, 102001 (2002)